Proc. Natl. Acad. Sci. USA
Vol. 94, pp. 7617–7620, July 1997
Neurobiology

Functional impact of cerebral connections

WIM VANDUFFEL*, BERTRAM R. PAYNE†, STEPHEN G. LOMBER†, AND GUY A. ORBAN*‡

*Laboratorium voor Neuro- en Psychofysiologie, Faculteit Geneeskunde, Gasthuisberg, Herestraat 49, B-3000 Leuven, Belgium; and †Laboratory for Visual Perception and Cognition, Department of Anatomy and Neurobiology, Boston University School of Medicine, 700 Albany Street, Boston, MA 02118

Communicated by James M. Sprague, University of Pennsylvania, Philadelphia, PA, May 1, 1997 (received for review March 13, 1997)

ABSTRACT **Cerebral networks are complex sets of connections that resemble a ladder-like web of multiple parallel feedforward, lateral, and feedback connections. This static anatomical description has been pivotal in guiding our understanding of signal processing within cerebral networks. However, measures on both magnitude and functional significance of connections are extremely limited. Here, we compare the anatomically defined strengths of a set of cerebral pathways emerging from the visual middle suprasylvian (MS) cortex of the cat with measures of the functional impact the same region has over distant sites. These functional measures were obtained by analyzing the local and distant effects of MS cooling deactivation on deoxyglucose uptake. Relative to major efferent projections from MS cortex that have a strong influence, projections to early visual processing stages have weaker functional influences than predicted from the anatomy. For higher processing stages, the converse holds: projections from MS cortex have stronger functional influence than predicted from the anatomy. We conclude that these and future functional measures, obtained using the same combination of techniques, will furnish fundamental, new information that complements and extends current models of static cerebral networks, and lead to more realistic models of cerebral network function and component interactions.**

The mammalian visual system consists of numerous anatomically and functionally defined cerebral cortical and subcortical components (1–5). For example in the cat, based on functional, architectonic, and connectional features, there are 19 visual cortical areas (5–7) and a number of subcortical structures that are interconnected by a large number of diverging and converging pathways (5–6). Also, based on varying levels of transported-label density in target structures, it is widely recognized that the anatomical strength of the connections between visual system components varies considerably. However, little effort to date has been expended to measure the strengths of the anatomical connections. Moreover, there is only limited information on the functional impact one region has over neurons in other regions (8, 9). In this study we (*i*) measured the anatomical strengths of projections for one efferent set of axons emerging from middle suprasylvian (MS) cortex, (*ii*) assessed the functional impact of these projections on target neurons, and (*iii*) compared the connectional strengths with the functional impacts. We chose MS cortex for our study because the region is accessible and because cooling has revealed that MS cortex plays a prominent role in visual processing, including orienting to targets (10, 11), pattern discrimination in the presence of moving masks (12, 13), and discriminations of differences in movement direction (13). In our study, connectional strengths were assessed by injecting tritiated amino acids into MS cortex and using standard autoradiographic pathway tracing techniques (14). Measures of functional impact were assessed by combining a global assay of neural activation levels using 2-deoxyglucose (2DG) (15–17) with localized cooling deactivation of MS cortex (8, 13). The comparison of the anatomical strengths with the functional impacts for several connections were largely in agreement. However, several significant differences were identified that pertain to both feedforward and feedback pathways.

MATERIALS AND METHODS

Cooling and 2DG Procedures. *Surgery.*§ In each of three cats, the MS sulcus of one hemisphere was opened using routine procedures (10, 12–13), a single loop of 23-gauge hypodermic tubing was permanently implanted, and the walls of the sulcus were allowed to close around the probe. In addition, an array of microthermocouples (Omega Engineering, Stamford, CT) was implanted in cortex adjacent to each probe to monitor temperatures of cortex (10). Surgeries were carried out under sterile conditions and after general anesthesia with ketamine (10 mg·kg^{-1} i.m.) and pentobarbital (20 mg·kg^{-1} i.v.). Antibiotics were administered (Natrium cefazolinum) for 1 week after surgery.

2DG administration. Four to six weeks later, the probes were cooled to 1°C by circulating chilled methanol through the tubing. Beginning 5 min after temperature stabilization (≈10 min after onset of cooling), one dose of 100 μCi·kg^{-1} 2-deoxy-D-[U-^{14}C]glucose (American Radiolabeled Chemicals, specific activity 55 mCi·mmol^{-1}) was injected (i.v.) over a 2-min period. The cats were fully conscious throughout to maximize 2DG uptake (18), and their bodies comfortably restrained in a box with form-fitting baffles. They observed the activities of a normal laboratory and were free to move their head and eyes. After 45 min elapsed, to ensure virtually complete 2DG uptake, heparin (2,500 units) and an overdose of sodium pentobarbital (50 mg/kg) were injected i.v.

Tissue fixation and preparation. The vascular system was flushed with a saline solution containing 15% sucrose, and the brain was fixed with 4% paraformaldehyde, 1.5% glutaraldehyde in a solution of 15% sucrose in 0.1 M phosphate buffer. Thereafter, the brain was quickly removed, frozen, and stored at −70°C (7). Thirty-five-micrometer-thick cryostat sections were cut at −20°C, mounted on coverslips, and dried at 50°C. The coverslips were secured with glue, sections outermost, onto boards. The sections and ^{14}C microscales (Amersham) were opposed to Agfa-Gevaert Structurix D7 film and stored in cassettes, in the dark, at −70°C. After 4 weeks, the films were developed with Kodak D-19 and fixed.

Anterograde Pathway Tracer Administration. *Surgery*§. In four cats, using surgical procedures similar to those described above, 100 μCi of a cocktail of L-[2,3,4,5-^{3}H]proline and L-[4,5-^{3}H]leucine was injected at six sites (A5, 8, and 11,

The publication costs of this article were defrayed in part by page charge payment. This article must therefore be hereby marked "*advertisement*" in accordance with 18 U.S.C. §1734 solely to indicate this fact.

Abbreviations: MS, middle suprasylvian; 2DG, 2-deoxyglucose; pCG, posterior cingulate cortex; CVA, cingulate visual area.

‡To whom reprint requests should be addressed. e-mail: Guy.Orban@med.kuleuven.ac.be.

§All surgical procedures were carried out in accordance with United States and European guidelines and regulations.

superficial and deep sites at each) in each of the medial and lateral banks of the MS sulcus.

Tissue fixation and preparation. After 1 week for uptake and transport, the animal was deeply anesthetized as described above, and the brain was fixed with formaldehyde, dehydrated, and embedded in a mixture of paraffin wax and plastic. Coronal sections were cut, mounted, deparaffinized, deplasticized, coated with Kodak NTB4 emulsion, and prepared for autoradiography using standard procedures (14). After a 4-week exposure period, silver grains were developed with Kodak D-19 and fixed. Subsequently, tissue sections were stained, through the emulsion, with thionin, dehydrated, and coverslipped using DePeX (Gurr, London) as a mountant. The four cats injected with tritiated amino acids revealed very similar qualitative results. Strength of the anatomical connections was assessed by measuring optical density of silver grains deposited by transported ^{3}H using the same sample procedures as described for the measurements of the 2DG concentrations. The contralateral auditory cortex, which receives no fibers from MS cortex, was used to define baseline optical density (zero-point).

Image Analysis. 2DG autoradiographs were digitized using a computerized imaging system (Analytical Imaging Concepts, Montreal). Images were corrected for inhomogeneities of illumination by image subtraction of the background. Using the calibrated microscales, gray values were converted in isotope concentration (7). Sample areas were 200 × 200 μm (2) and separated by ≈150 μm, and extended through a structure but ignoring boundary regions. Between 120 and 820 measurements per structure were made. In cerebral cortex these measures were made independently in the upper, middle, and lower thirds of the cortical thickness. Functional measures of the impact of the cooling deactivation were calculated by comparing averaged 2DG concentrations in structures in the cooled hemisphere and at homotopic sites in the noncooled hemisphere. Data of the three cats were pooled. This procedure potentially underestimates the identified cooling-induced effects that may be transmitted through cerebral commissures to homotopic sites. ANOVA revealed that all effects on 2DG uptake in the cooled hemisphere are significantly different from values obtained for the noncooled hemisphere ($P < 0.05$). Exceptions are all layers of lateral geniculate nucleus, medial and upper layers of area 18 (18 m and 18 u), the ventral half of the putamen, and all regions of auditory cortex.

RESULTS

Fig. 1*A* shows that 2DG uptake in MS cortex in contact with the cryoloop was very low, and similar to white matter uptake, when the cryoloop was cooled to 1°C. Moreover, strong effects of the cooling penetrated through all or most of the cortical thickness. Reconstruction from a series of coronal sections shows a close-fitting envelope of low DG uptake around the probe. In this cat, the region extended from coronal level A2 to A15 and encompassed most of areas AMLS and ALLS and the anterior two-thirds of areas PMLS and PLLS of Palmer *et al.* (20).

Inspection of 2DG autoradiograms reveals that the silencing of MS neurons (10, 12) diminishes 2DG uptake in a number of specific and distant regions in both cortex and thalamus. The most obvious decreases in 2DG uptake in the cooled hemisphere (compared with the noncooled hemisphere) were in areas pCG (posterior cingulate), CVA (cingulate visual area), splenial visual area, deep area 18 and medial area 19, and the full thickness of fundal area 19. In thalamus, diminished uptake was evident in regions within the pulvinar and lateral posterior nuclei (Fig. 1*B*). Quantification of 2DG uptake verifies these observations and identifies cooling-induced decreases in 2DG uptake in these and other cortical and subcortical structures. A range of such effects are observed (Fig. 3 ordinate). Importantly, these effects are not related in any systematic way to distance from the cooling probe ($r = -0.23$, $P = 0.19$). In fact, uptake of 2DG in auditory cortex only 2–3 mm from the probe (Fig. 1*A*), as well as numerous other structures not linked to efferent MS pathways, are unaffected by the cooling.

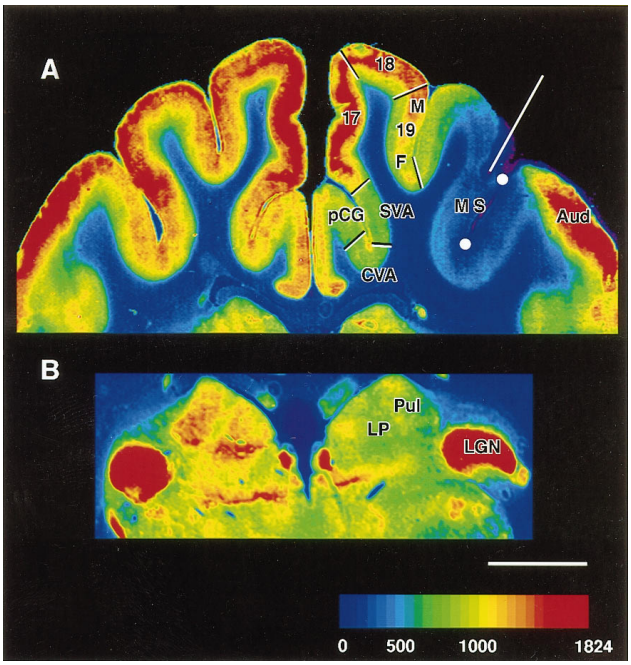

FIG. 1. Color-coded image of 2DG concentration in coronal sections of cerebral cortex (*A*) and dorsal thalamus (*B*) during cooling deactivation of cortex lining the MS sulcus. White circles in MS sulcus represent position of the cooling probe. Red line indicates trajectory of one of the thermocouples used to measure the temperature of the cooled cortex. Temperature of cortex at indicated site was 15°C, a temperature that blocks neuronal activity but not conductivity (19). Color scale represents [^{14}C]2DG concentration (nCi·g^{-1}). White scale bar represents 5 mm. SVA, splenial visual area; Aud, auditory cortex; LGN, lateral geniculate nucleus; Pul, pulvinar nucleus; LP, lateral posterior nucleus; 17, 18, areas 17 and 18; 19M, 19F, area 19 medial or fundal parts.

To support our contention that the diminished 2DG uptake at selected distant sites reflects the silencing of signals emanating from the MS region, we investigated the topographic match between lowered 2DG uptake during cooling and efferent projections from MS cortex. For the tracer study, we injected tritiated amino acids into both banks of the MS sulcus and took great care to expose to tracer a region of cortex that mimics the one inactivated during cooling. There was a 92% congruence between the two techniques. We assessed the congruence of the region cooled and showing a decrease in 2DG uptake with the region exposed to pathway tracer. For the assessments, which were made at four coronal levels, continuous sequences of 2DG concentration and pathway tracer density measurements were made along cortical layer 4 from medial area 17 through MS cortex to auditory cortex. Using the sequential borders between areas 17, 18, 19, and 7 MS cortex, and auditory cortex as guides, we aligned sets of measurements at each coronal level for the two groups of cats. For both the pathway tracer densities and the 2DG concentrations we concentrated on identifying the positions of medial and lateral transition zones from low to high pathway tracer density and vice versa, and high to low 2DG concentration and vice versa. In the intervening region, comprising both banks of MS sulcus, the pathway tracer density was homogenous and high, and the cooling induced decrease in 2DG concentration was homogeneous and low.

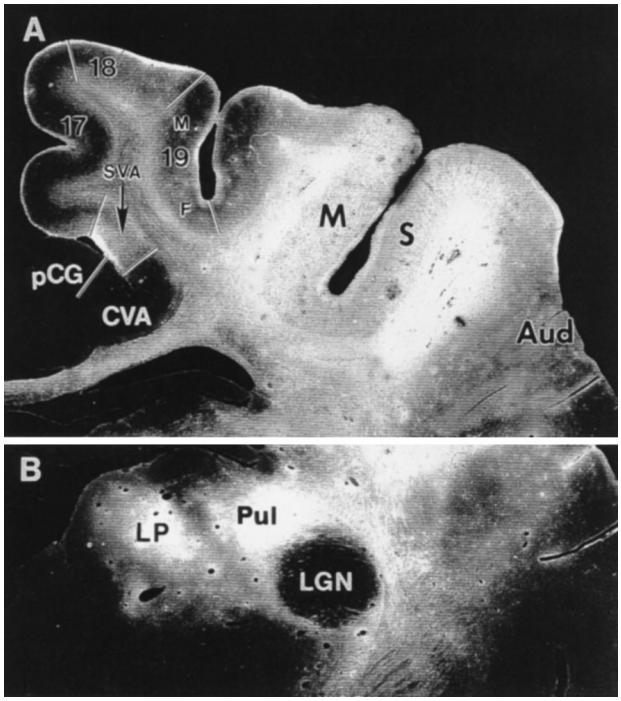

FIG. 2. Distribution of [^{3}H] proline and [^{3}H] leucine mixture at the injection site in cortex lining the MS sulcus and after transport to cortical (*A*) or thalamic (*B*) targets. Darkfield illumination. Region exposed to tracers extends from A3 to A13. (*A*) Note distribution of transported label and absence of label from areas pCG and CVA. SVA, splenial visual area; Aud, auditory cortex; LGN, lateral geniculate nucleus; Pul, pulvinar nucleus; LP, lateral posterior nucleus; 17, 18, areas 17 and 18; 19M, 19F, area 19 medial or fundal parts.

In MS cortex, the density of tritiated amino acids is uniform (Fig. 2*A*) and, in agreement with previous reports (6, 21–26), efferent projections of variable density were identified in a number of target structures (Figs. 2 and 3 abscissa). However, label was not detected in areas pCG, CVA, and subdivisions of a number of subcortical structures, such as the claustrum and the putamen, where cooling diminished 2DG uptake. Some of these areas and structures are linked to MS cortex by a limited number of intermediary stations. For example, efferent signals from MS cortex can reach pCG via either areas 7 (6) or splenial visual area (27).

There is a clear relationship between decreased 2DG uptake and efferent projections from MS cortex ($r = 0.48$, $P = 0.003$). Even so, the variation in connection strength explains only 23% of the variation in decreased 2DG uptake. To investigate this quantitative mismatch further, we chose to standardize our comparison between the 2DG and the tracer study by equating cooling-induced changes in 2DG concentration with the density of tracer in the pulvinar nucleus, a structure both strongly influenced by cooling of MS cortex and receiving dense anatomical projections from the same region (26). For a number of other structures, the standardizing procedure reveals equally strong tracer density and cooling-induced effects on 2DG concentration (Fig. 3 diagonal). However, for several other structures there are significant discrepancies between tracer density and cooling effect. Points falling below the diagonal in Fig. 3 have a lower cooling effect than would be predicted on the basis of anatomical strength of connections. The mismatch in this direction is characteristic of structures involved in the early processing of visual signals (blue/green color code in Fig. 3). Conversely, points above the diagonal indicate a cooling effect greater than predicted from the density of anatomical connections. These structures occupy either a higher position in the cerebral hierarchy or are located

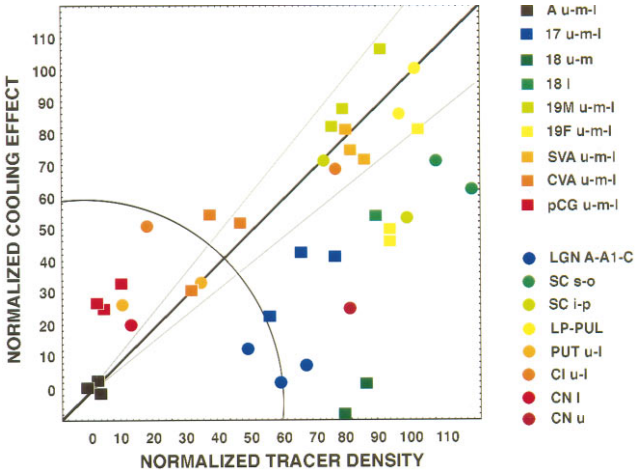

FIG. 3. Graph of normalized tracer density versus normalized cooling effect on 2DG concentration for a variety of cortical and subcortical structures. Normalization based on equating tracer density and decrease in 2DG uptake in contralateral auditory cortex to 0% and in the pulvinar nucleus to 100%. Solid line represents slope of unity that indicates that tracer density and effects on 2DG uptake are equal. Gray lines represents 20% deviation from these values. Squares represent cortical structures. Circles represent subcortical structures. The color-coded label for the different structures reflects levels of visual processing: blue, early; green/yellow, intermediate; and red, late. Radial distance represents connection strength, independent of measurement method, whereas polar angle (quarter circle) reflects the balance between functional (2DG) and anatomical (tracer) measurements of the connection. Points below the diagonal show a weaker 2DG effect than anticipated from the anatomy whereas points above the diagonal show a stronger 2DG effect than anticipated from the anatomy. Choice of another structure for normalization of measurements (e.g., area 17 rather than pulvinar) alters the number of points above and below the line but do not change the order of the points along the polar dimension. Hence conclusions are not affected by our choice of the pulvinar to equate functional and anatomical measurements. SVA, splenial visual area; 17, 18, areas 17 and 18; 19M, 19F, area 19 medial or fundal parts; Aud, auditory cortex; LP, lateral posterior nucleus; Pul, pulvinar nucleus; LGN A, A1 and C, lateral geniculate nucleus A, A1, and C subdivisions; PUT l and u, putamen lower and upper; CN l and u, caudate nucleus lower and upper; Cl l and u, claustrum lower and upper; SC s, o, i, and p, superior colliculus superficialis, opticum, intermediale, and profundum.

at the interface with the motor system (yellow/red color code in Fig. 3) (6).

We recognize that equating the two measures in pulvinar may be artificial, and the relationship between both measures might be nonlinear. However, selection of any other structure for the equalization procedure, which both receives strong projections from MS cortex and shows significant cooling induced modulations, does not alter our conclusions in any material way; and there are structures with virtual no cooling effect on DG uptake showing high tracer uptake (e.g., area 18) or vice versa (e.g., CVA and pCG). In these instances, the linearity between both measures is unimportant.

DISCUSSION

Overall, our results show that cooling of MS cortex specifically reduces metabolic activity in a number of cerebral cortical areas and subcortical structures that can be linked with the cooled region, either directly or via a limited number of intermediary stations and connections. This conclusion is reached regardless of normalization method used. Even so, the strength of the functional links revealed with reduced uptake of 2DG only partially match the strength of the anatomical connections. For example, the influences of MS cortex on early stations in the visual pathway are weaker than anticipated from

the anatomical data. In contrast, for higher stations, or stations more closely linked to motor responses, the functional influences of MS cortex are relatively stronger than predicted from the anatomy. Moreover, these forward influences can extend beyond one linkage to even higher-order regions that are not directly connected with MS cortex. Thus, cooling combined with 2DG reveals the functional impact of anatomical connections on neural activity that cannot be predicted from standard wiring diagrams of the cerebral network.

In these analyses, it is important to recognize that the cats were in a passive viewing mode, and this might explain, in broad terms, that the relative strength of the functional impacts reflects the anatomically defined hierarchy. For example, at early levels of visual processing, strong visual inputs may overshadow feedback connections that have only relatively modest functional impact; whereas regions beyond MS cortex or at the interface with motor systems may depend on MS cortex for much of their activity and the functional impact is greater. One can posit that under less passive conditions the functional state of the system may deviate significantly from this default mode as attentional and mnemonic influences originating from higher areas modify activity levels at earlier stages of processing (28–33). Moreover, it may well be that these higher-order cerebral influences can be captured and localized with this combination of cooling and 2DG. Also, the method may provide functional measures of the flexibility of cerebral connections and indicate flow of signals through the network under a variety of behavioral conditions. These measures are likely to complement current concepts of cerebral networks based on static anatomy, and they are likely to substantially advance our understanding of neural networks and provide links to perceptual and cognitive aspects of brain function. Finally, the method also may be useful for assessing changes in the functional weight of connections as a result of neural compensations after restricted lesions of cerebral network components. These assessments can be made by comparing the functional impact of localized cerebral cooling with the functional impact of ablating an equivalent cerebral region in another animal. Such comparisons are likely to provide valuable information on the functional plasticity of cerebral network components and sites of lesion-induced neural compensations (8).

We thank Roger Tootell for use of his cryostat and imaging equipment. We are grateful to Sarah Geeraerts, Gerrit Meulemans, and Piet Kayenberg for technical assistance. We also thank the National Institutes of Health, Flemish Regional Ministry of Education (GOA 95/6), National Research Council of Belgium (NFWO G3106.94), and Belgian State Prime Minister of Science Policy Programming (IUAP nr. 22) for financial assistance.

1. Van Essen, D. C., Andersen, C. H. & Felleman, D. J. (1992) *Science* **255,** 419–423.
2. Boussaoud, D., Ungerleider, L. G. & Desimone, R. (1990) *J. Comp. Neurol.* **296,** 462–495.
3. Van Essen, D. C. & De Yoe, E. A. (1995) in *The Cognitive Neurosciences*, ed., Gazzaniga, M. S. (MIT Press, Cambridge, MA), pp. 383–400.
4. Young, M. P. (1992) *Nature (London)* **358,** 152–155.
5. Tusa, R. J., Palmer, L. A. & Rosenquist, A. C. (1981) in *Cortical Sensory Organization*, ed., Woolsey, C. N. (Humana, Clifton, NJ), Vol. 2, pp. 1–31.
6. Rosenquist, A. C. (1985) in *Cerebral Cortex*, eds., Peters, A. & Jones, A. G. (Plenum, New York), Vol. 3, pp. 81–117.
7. Vanduffel, W., Vandenbussche, E., Singer, W. & Orban, G. A. (1995) *J. Comp. Neurol.* **354,** 161–180.
8. Payne, B. R., Lomber, S. G., Villa, A. E. & Bullier, J. (1996) *Trends Neurosci.* **19,** 535–542.
9. Orbach, H. S. & Van Essen, D. C. (1993) *Exp. Brain Res.* **94,** 371–392.
10. Payne, B. R., Lomber, S. G., Geeraerts, S., Van der Gucht, E. & Vandenbussche, E. (1996) *Proc. Natl. Acad. Sci. USA* **93,** 290–294.
11. Lomber, S. G. & Payne, B. R. (1996) *Visual Neurosci.* **13,** 1143–1156.
12. Lomber, S. G., Cornwell, P., Sun, J. S., MacNeil, M. A. & Payne, B. R. (1994) *Proc. Natl. Acad. Sci. USA* **91,** 2999–3003.
13. Lomber, S. G., Payne, B. R., Cornwell. P. & Long, K. D. (1996) *Cereb. Cortex* **6,** 673–695.
14. Payne, B. R., Pearson, H. E. & Cornwell, P. (1984) *Proc. R. Soc. London Ser. B* **222,** 15–32.
15. Sokoloff, L., Reivich, M., Kennedy, C., Des Rosiers, M. H., Patlak, C. S., Pettigrew, K. D., Sakurada, O. & Shinohara, M. (1977) *J. Neurochem.* **28,** 897–916.
16. Tootell, R. B. H., Hamilton, S. L., Silverman, M. S. & Switkes, E. (1988) *J. Neurosci.* **8,** 1500–1530.
17. Vanduffel, W., Vandenbussche, E., Singer, W. & Orban, G. A. (1997) *Eur. J. Neurosci.*, in press.
18. Löwel, S. & Singer, W. (1993) *Eur. J. Neurosci.* **5,** 857–869.
19. Bénita, M. & Condé, H. (1972) *Brain Res.* **36,** 133–151.
20. Palmer, L. A., Rosenquist, A. C. & Tusa, R. J. (1978) *J. Comp. Neurol.* **177,** 237–256.
21. Musil, S. Y. & Olson, C. R. (1988) *J. Comp. Neurol.* **272,** 203–218.
22. Abramson, B. P. & Chalupa, L. M. (1985) *Neuroscience* **15,** 81–95.
23. Harting, J. K., Updyke, B. V. & Van Lieshout, D. P. (1992) *J. Comp. Neurol.* **324,** 379–414.
24. Updyke, B. V. (1993) *J. Comp. Neurol.* **327,** 159–193.
25. LeVay, S. & Sherk, H. (1981) *J. Neurosci.* **1,** 956–980.
26. Updyke, B. V. (1981) *J. Comp. Neurol.* **201,** 477–506.
27. Maekawa, H. & Ohtsuka, K. (1993) *Neurosci. Res.* **17,** 315–323.
28. Corbetta, M., Miezin, F. M., Dobmeyer, S., Shulman, G. L. & Petersen, S. E. (1991) *J. Neurosci.* **11,** 2383–2402.
29. Fink, G. R., Halligan, P. W., Marshall, J. C., Frith, C. D., Frackowiak, R. S. J. & Dolan, R. J. (1996) *Nature (London)* **382,** 626–628.
30. Orban, G. A., Dupont, P., Vogels, R., Bormans, G. & Mortelmans, L. (1997) *Eur. J. Neurosci.* **9,** 246–259.
31. Motter, B. C. (1994) *J. Neurosci.* **14,** 2178–2189.
32. Treue, S. & Maunsell, J. H. R. (1996) *Nature (London)* **382,** 539–541.
33. Luck, S. J., Chelazzi, L., Hillyard, S. A. & Desimone, R. (1997) *J. Neurophysiol.* **77,** 24–42.